CRYSTAL CHEMISTRY OF OLIVINES AND GARNETS IN ALPINE ULTRAMAFICS: INFORMATION CONTRIBUTED BY XAFS

MOTTANA, A.*, PARIS, E.**, MARCELLI, A.***, WU, Z.**** & GIULI, G.*****

* Università di Roma Tre, Dipartimento di Scienze Geologiche, Via Ostiense 169, I-00154 Roma RM, Italy
** Università di Camerino, Dipartimento di Scienze della Terra, Via Gentile III da Varano, I-62032 Camerino MC, Italy
*** Istituto Nazionale di Fisica Nucleare, Laboratori Nazionali di Frascati, Via Enrico Fermi 40, I-00044 Frascati RM, Italy
**** Institut des Matériaux de Nantes, C.N.R.S.-U.M.R. 110, 2 rue de la Houssinière, F-44072 Nantes Cedex 03, France
***** Università di Firenze, Dottorato di Ricerca in Mineralogia e Petrologia, Via Giorgio La Pira 4, I-50121 Firenze FI, Italy

Abstract
The XANES experimental and calculated spectra of olivine and pyrope are discussed with reference to natural samples occurring in the alpine ultramafics. The potential of XAFS as a tool to investigate short-range-order around a selected atom chosen as the absorber is pointed out.

Introduction
X-ray Absorption Fine Structure (XAFS) spectroscopy was discovered in the early '20s (FRICKE, 1920; HERTZ, 1920; KRONIG, 1921), but it became of interest as a technique suitable to study the properties of solid materials only in the late '60s, when synchrotron radiation started being used as the appropriate X-ray source to generate spectra having a good enough signal to noise ratio.

At that time SAYERS et al. (1970, 1971) and STERN (1974) developed the theoretical background and the practical technique of EXAFS (Extended X-ray Absorption Fine Structure), thus making it possible to retrieve quantitative information about the atomic shells around the excited atom (absorber) from the analysis of undulations occurring in the high-energy part of XAFS spectra.

By contrast, XANES (X-ray Absorption Near Edge Structure), the portion of the spectrum which is the most intense one and had been noticed first, remained poorly explained till well within the '80s, although it was widely used to extract information about the local structure around the absorber via an empirical method known as »fingerprinting« technique. Only in recent years a full theoretical treatment of XANES has become available, which is based on the long-since known one-electron multiple-scattering (MS) theory first conceived by LEE & PENDRY (1975). Theory and practice were developed over the years by NATOLI and co-workers (1980, 1986, 1990) and DURHAM et al. (1982). Finally, the comprehensive formalism embodied in the CONTINUUM code of NATOLI et al. (1990), with additional modifications by TYSON et al. (1992), has now created the conditions to make XANES a most po-

werful tool to quantitatively investigate local structure, namely the site geometry around the atom chosen as absorber.

It is indeed worth pointing out what the properties of XANES are, so as to compare them with XRD, the much more widely known and commonly used X-Ray Diffraction method to study crystal structure.

When an X-ray beam impinges a solid, it is either diffracted or absorbed. Diffraction occurs when the X-rays are being scattered by the outer electron cloud of the impinged atom with their wavelength remaining unmodified; in such a case some of the waves coherently originating from nearby atoms will interfere positively and give rise to Bragg reflections. If scattering occurs incoherently under modified (longer) wavelengths (Compton scattering), then only a diffuse background is being produced. Absorption occurs when the X-rays impinging the atom have energy such as to force electron transitions in the inner shells. The ejection of an electron from the innermost K shell (*1s* electron) involves the strongest energy and produces the K-edge spectrum characteristic of the atom.

In detail, such an element-specific XAFS spectrum consists of three sections (NATOLI & BENFATTO, 1986): (i) the pre-edge, which represents the onset of electronic transitions from the 1s core level to the lowest-energy unoccupied levels of the atom, and mostly consists in a single sharp or poorly structured and weak peak; (ii) the XANES region, which is due a process of ionization of the core electron to a delocalized energy band, or to its complete ejection from the atom; according to the MS theory, the ejection process is not simple, but involves many-path interactions with the neighbouring atoms, thus generating a series of perturbations onto the strong peak marking the main absorption (white-line); (iii) the EXAFS region, which consists of smooth undulations (ripples) superimposed on the declining tail of the edge arising from single-scattering of the outgoing photoelectron with neighbouring atoms; the undulation frequency is reciprocally related to interatomic distance, and the amplitude to the number of nearest neighbours (coordination).

Absorption is a much more energy-consuming process than diffraction is, because the involved photoelectrons have their mean free paths necessarily limited in their scattering by the surrounding atoms. Consequently absorption fades out rapidly within a short distance from the excitation point, in contrast to diffraction, which involves photons which are elastically scattered over a much longer distance. Till a few years ago it was believed that XAFS could inform at most about 3–4 coordination shells around the absorber (i.e., 4–5 Å). Our own calculations indicate that the multiple-scattering process may extend much farther depending on the arrangement of the neighbours around the absorber i.e., on crystal symmetry; e.g., to reproduce the XANES spectrum of a monoclinic mineral like diopside 58 atoms were enough i.e., all the atoms in a sphere 6 Å in radius (PARIS et al., 1995), but for a cubic mineral like periclase the agreement between calculation and experiment becomes good only when more than ca. 100 atoms are considered i.e., a sphere 8–9 Å in radius (WU et al., 1996a). Thus, although a less local probe than it was believed a few years ago, XAFS gives an information which is much more localized than the one given by XRD, where the diffraction process involves a width of some 200–300 Å.

As a conclusion; information contributed by XAFS concerns the short-range-order (SRO) relationships existing between an atom and its neighbours, and complements most effectively that on long-range-order (LRO) contributed by XRD. The added value of XAFS lies in that it is element-specific i.e., it concerns only the environment of the element which is being excited by modulating the energy of the impinging X-ray beam, whereas XRD averages contributions from all atoms located over the entire lattice portion which is illuminated by the X-rays. This makes XAFS an invaluable tool for studying chemical substitutions in minerals, and especially for locating the positions where trace elements substitute for major elements.

Methods

Most experimental results referred to in the following sections have been obtained at Stanford Synchrotron Radiation Laboratory (SSRL) on beamline SB03-3 equipped with the Jumbo monochromator and the novel YB_{66} crystal, which is optimized for spectroscopy in the 1–2 KeV range i.e., it covers the Mg, Al and Si K-edges (WONG et al., 1994). Additional results were obtained on beamline SB04–1 equipped with a Lytle detector for the minor elements Fe, Ni, Mn, and Co. Calculations were performed at Laboratori Nazionali di Frascati (LNF) using C.R. Natoli's CONTINUUM package of programs with the latest additions. Details on both data acquisition and data processing will be reported elsewhere.

Results

Olivine. An olivine solid solution ca. $Fo_{90}Fa_{10}$ is the main constituent of the Earth's Mantle at depths where basaltic magmas form by partial melting. At the surface this olivine may be sampled in at least four types of ultramafics: **a)** granular peridotite nodules in oceanic basalts outpouring at diverging plate margins; **b)** tectonitic peridotite to lherzolite slabs obducted where the Upper Mantle is squeezed upwards inbetween two colliding plates; **c)** circumscribed lherzolite to harzburgite bodies emplaced along deep regional faults in the root-zone of mountains chains; and **d)** sheared peridotite nodules carried by kimberlite pipes. In the Alps, type **a** is to be found rarely (e.g. in the Lessini volcanic area); type **b** is widespread (e.g. Voltri, Finero, Malenco); type **c** is also rather common (e.g. Lanzo, Balmuccia). A rather special occurrence is Alpe Arami, long since believed to belong to type c (MÖCKEL, 1969), later related to eclogite-facies metamorphism of an ultrafemic protolith (HEINRICH, 1986) together with other alpine occurrences such as Nonsberg, and most recently re-interpreted as an intrusion from the very deep Mantle, possibly from the Asthenoshere (DOBRZHINETSKAYA et al., 1996) i.e., much the same as type **d** above.

We have approached the olivine problem by calculating first the theoretical Mg and Fe K-edge spectra for the endmembers, and by comparing them with experimental spectra (WU et al., 1996a). Then we measured the spectra for quite a few olivines including a number from alpine occurrences, and compared them with the endmembers, thus deducing their status of chemical substitution and the ensuing local order.

In order to adequately reproduce the experimental spectra of endmember olivines Fo_{100} and Fa_{100}, the contributions of the two octahedral cation sites **M**1 and **M**2 (present in the structure together with the tetrahedral T site) must be calculated separately, using clusters which require up to 89 atoms to reach convergence; the olivine full spectrum

is the sum of the two cluster spectra, thus containing ca. 180 atoms and extending to ca. 20 Å away from the absorber (WU et al., 1996). Whith this result achieved, the fine features superimposed on the edgetop in the experimental spectra can be deconvoluted, in the sense that they can related to contributions arising from different MS paths of the ejected photoelectron when it collides with the absorber neighbours.

The experimental Fo_{100} Mg K-edge spectrum (Fig. 1) is very well resolved, and shows as many as four features in the Full Multiple Scattering (FMS) region extending to +10 eV above the edge, two others in the Intermediate Multiple Scattering (IMS) region i.e. from +10 to +40 eV, and two final ones which lie in the region where Single Scattering (SS) merges with EXAFS undulations. The Fa_{100} Fe K-edge spectrum exhibits the same number of features as the forsterite one, but it is definitively less resolved. It is unclear on whether this is due to some intrinsic property of the material (CALAS et al., 1988: the fayalite used is not explained) or to poor resolution of the apparatus; we incline to believe that CALAS et al. (1988) operated with an excellent apparatus, however on a synthetic fayalite having poor internal crystallinity: indeed previous fayalite spectra by WAYCHUNAS et al. (1983) are even worse. CALAS et al.'s (1988) fayalite spectrum exhibits a small but definite pre-edge, in agreement with the fact that Fe contains numerous empty levels where the photoelectron can be ejected to. Despite these uncertainties, even in this fayalite spectrum the contributions to each individual feature can be deconvoluted and assigned; this offers the way to consistently identify the arrangement of the scattering atoms around the absorber: local SRO, in other words.

The Mg K-edge of an intermediate olivine changes whith changing atoms in the octahedral sites. For simplicity, we assume that our sample Fo_{50}, being a synthetic product quenched from very high temperature (1400°C), is fully disordered i.e., it has a completely statistical Fe-Mg distribution in both **M1** and **M2**. Its Mg K-edge spectrum is not as well resolved as the Fo_{100} spectrum was, yet the major characteristics can still be recognized in the FMS region; the largest differences are in the IMS and SS regions, thus suggesting that EXAFS, rather than XANES, would be able to give better information contributing to understanding of SRO in this sample. By contrast, a fully ordered natural monticellite, where Mg is totally partitioned in **M1** and Ca equally partitioned in **M2**, has a rather poor Mg K-edge spectrum: the edge itself is still there, but the fine features which would permit characterizing SRO can no longer be seen.

Olivines from alpine ultramafics give excellent evidence for the above behaviour. The Mg K-edge spectrum of olivine in the Lessini peridotite nodule ($Fo_{89.5}Fa_{10.3}Te_{0.2}$) (Fig. 1) is almost identical as the Fo_{100} reference forsterite; the major changes are in the smoother outline of the edgetop, where peak D tends to desappear, and the near complete desappearence of peak E; by contrast hump G in the IMS region is stronger than it was in Fo_{100}. The Malenco olivine ($Fo_{85.7}Fa_{14.0}Te_{0.3}$) (Fig. 1) is essentially similar, although being slightly different in composition. By contrast, the Alpe Arami olivine ($Fo_{90.1}Fa_{9.8}Te_{0.1}$) (Fig. 1) shows peculiarities of its own, such as peaks A and D much better resolved, peaks B lacking, and reduction of humps E and G. Clearly, this different spectrum implies crystal chemical differences at a local scale, in as much as the bulk composition of the Alpe Arami olivine is practically identical to that of the Lessini one.
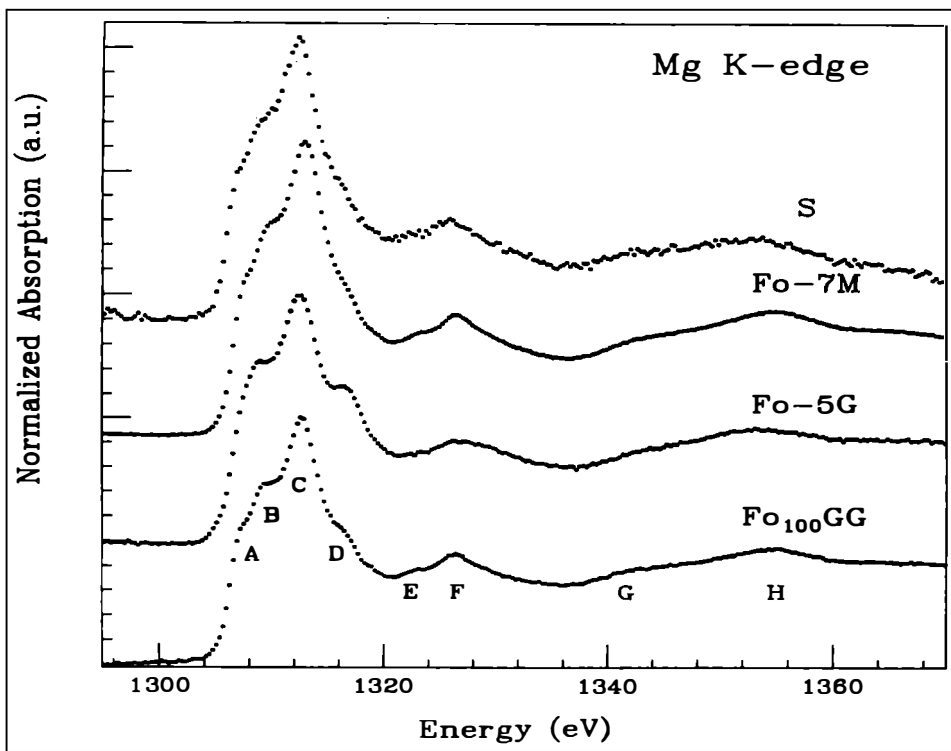
Fig. 1:
Mg K-edge XANES spectra of olivines in alpine ultramafics (from top to bottom): S = Lessini nodule; Fo–7M = malenco serpentine; Fo–5G = Alpe Arami lherzolite; $Fo_{100}GG$ = synthetic forsterite.

WU et al.'s (1996a) decomposition of the olivine XANES spectrum, together with a meaningful application of NATOLI's rule, give the clues needed to relate the observed differences to changes in the atomic environment around the Mg absorber. Peak A mainly arises from contributions from the **M2** site; peak B and shoulder D arise mostly from **M2** again, whereas edgetop C reflects contributions from both **M1** and **M2**. Using NATOLI's rule, we relate A to the longest octahedral distance **M2–O31**; B to to the second longest **M2–O12**; C to the nearly equal short bonds **M1–O12 + M1–O22 + M2–O32**, and finally D to the shortest bond **M2–O21**. Note that the edgetop sums up contributions from three almost identical interaction paths, its intensity thus reflecting the multiple chance for the photoelectron to follow paths which are differently oriented yet equivalent in length.

The strong shoulder A in the Alpe Arami olivine spectrum speaks for a stronger interaction between the Mg absorber and the oxygen located in **O31**, as well as with the one in **O21**; thus, being this Mg located in **M2**, it also speaks for partitioning of the available Fe in **M1**. This explains, in turn, why edgetop C is not as sharp as it was in the other

39

olivines, but it tends to open up and display its triple composition. Finally, the strong peak D points out, in addition to A, the substantial preference of Mg for **M**2.

Concluding; XAFS spectroscopy for these typical olivines in alpine ultramafics indicate different crystal chemical relationships at the very local scale, down to a volume encompassing 2–3 unit cells. It is now up to petrologists to explain these findings with appropriate P–T–t-models.

Garnet
There are not many garnet-bearing ultramafics in the Alps, and samples of only few of these are such as to permit XAFS measurements. Consequently, we will describe the results obtained essentially on one sample (Alpi Arami), but only after having shown the properties of XAFS by referring to the extreme case of the pyrope from Parigi, Dora-Maira Massif (CHOPIN, 1984), grown under extreme P in either a whiteschist or a granitoid.

The general formula of cubic garnets is $X_3Y_2Z_3O_{12}$, where X = Mg, Fe, Mn, Ca within 8-fold coordinated dodecahedra, Y = Al, Cr, Fe within octahedra, and Z = Si in tetrahedral sites. We will discuss here the crystal-chemical relationships we determined for Mg and Al, as representative of the Prp component of garnet that is most interesting for ultrafemic compositions; however, our best results were obtained for Grs i.e., the garnet endmember containing the atoms having largest size difference, consequently displaying the best resolved spectrum (WU et al., 1996b).

The Mg K-edge spectra for the Dora-Maira pyrope show small changes which underline small differences in composition. The purest sample ($Prp_{97.6}Alm_{0.2}Grs_{0.2}$) is the pink, translucent, gem-quality intermediate rim of a porphyroblast 6 cm in diameter. Its XANES spectrum (Fig. 2) consists of a shoulder in the raising slope to the edgetop followed by a very weak shoulder down-slope in the FMS region, and of several weak humps in the IMS region. This experimental spectrum does not compare too well with the theoretical spectrum, which required as many as 83 atoms (cf. CHABOY & QUARTIERI, 1995) to attain convergence. However, when the cluster reaches this size, the calculated spectrum is much better resolved and in fact shows the first feature as separate peak rather than as shoulder.

The Mg K-edge spectrum of the Alpe Arami pyropic garnet ($Prp_{70.6}Alm_{16.3}Grs_{12.3}Sps_{0.8}$) agrees better with the Dora-Maira pyrope than with the calculated one: the major difference is in the down-slope shoulder, which in the Alpe Arami sample is sligthly better resolved, but less intense, while the three humps in the IMS region are comparatively less distinct because of an unfavourable signal to noise ratio. As a whole, it appears that the significant Fe+Ca contents in this garnet make themselves recognizable by blurring somewhat the Mg K-edge spectrum.

The Al K-edge spectrum of Prp_{100} was simulated easily using a cluster of 49 atoms, and is consistent with the spectrum calculated for Grs_{100} (WU et al., 1996b) in that it displays the same five major features, A to E, plus a number of weaker features in the IMS region which are still far from being understood. The white-line B is particularly strong and overcomes all other features, e.g. A that shows up just as a shoul-

40

der on the raising slope of B. C is also very weak, as are all other features in the IMS region. In the Grs case (WU et al., 1996b) assigned peak B to Al transitions from *1s* to unoccupied p-like states, and peak A mainly to transitions towards Al *3p* states possibly mixed with the empty states of the second-shell atom, Ca, in particular those having *3d* character. We support the same model in the case of Prp_{100}, where shoulder A is extremely weak because Mg has no *3d* states. Furthermore, WU et al. (1996b) showed that peak A could be reproduced only with clusters including the fourth and fifth shell around the Al atom, and came to the conclusion that the final state reached in core transitions is not a simple atomic or molecular state, but it has to be sensitive to LRO effects.
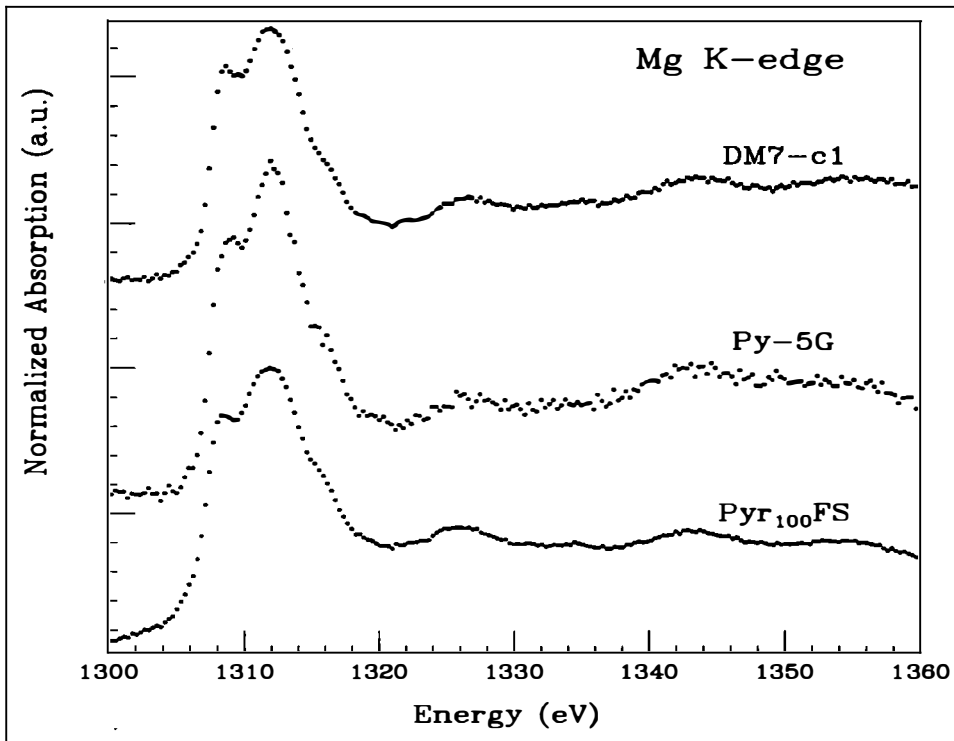

Fig. 2:
Mg K-edge XANES spectra of pyropic garnets in alpine ultramafics (from top to bottom): DM7–c1 = Dora Maira pyrope; Py–5G = Alpe Arami pyropic garnet; $Pyr_{100}Fs$ = synthetic pyrope.

When we compare our calculated Prp_{100} Al K-edge spectrum with the experimental spectrum of Dora-Maira pyrope (Fig. 3), we immediately see that peak A is much stronger than expected, as are all peaks in the IMS region from C onwards, despite being still weak. We explain this as due to a compositional effect: the Dora-Maira garnet, although the purest pyrope known so far, contains some Alm component although very little; given

41

the presence of several *3d* states in Fe, it is no wonder if A increases in intensity; on the other hand, the general weakness of the IMS region rules out the effect of Ca, because our Grs calculation would show this part of the spectrum to be proportionally rather enhanced if Ca were present. Apparently, Al in the Dora-Maira pyrope has mostly Mg as its second-shell neighbour, with only few but not negligeable Fe atoms spread rather sparsely as far as up to the fifth coordination shell.

The Alpe Arami pyropic garnet has an Al K-edge spectrum which is better resolved than the Dora-Maira one although displaying exactly the same number of features. In particular, in the FMS region, both the up-slope and the down-slope shoulder astride the white-line are distinctly separated from the main peak, thus underlying the higher amounts of cations in X other than Mg which interact with the Al ion located in Y and acting as the absorber.

As a conclusion; information from garnets at both the Mg and Al K-edges tend to underline the high purity and elevated structural order of the minerals examined, in agreement with their character of highly refractory phases little or not at all affected by structural dishomogeneity even at a local scale.
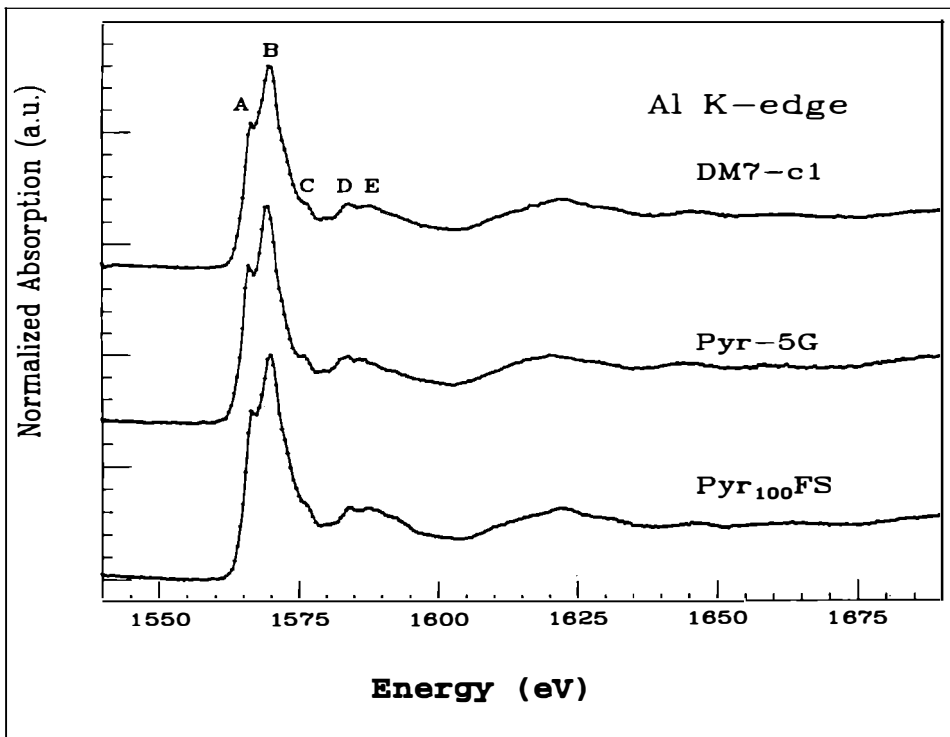

Fig. 3:
Mg K-edge XANES spectra of pyropic garnets in alpine ultramafics (from top to bottom): same samples as in Fig. 2.

Conclusions

Despite of its acknowledged potentials, XAFS is still a rather uncommon technique in the study of the crystal chemistry of minerals, and especially of rock-forming minerals. Yet, the combination of XANES experimental and calculated spectra shown here for olivines and garnets occurring in rocks of ultrafemic composition from the Alps suggests that greater attention should be given to this method to achieve deeper understanding of the local state of order, and consequently thermodynamic properties of these important mineral phases.

Evidence is given that the olivines in the Alpe Arami body, now re-interpreted to originate from very deep in the Mantle, possibly in the Asthenosphere, have their Mg and Fe distributed on a local scale according to an arrangement different from other alpine olivines also believed to originate from depth, however from the Upper Mantle.

Furthermore, the Prp-rich garnet of the Alpe Arami body shows Mg and Al local distributions which do not fit the distribution pattern of the Dora-Maira pyrope, which is indeed formed in a non-ultrafemic composition (a whiteschist or a meta-granitoid), but it is the product of subduction metamorphism at or very near the deepest conditions witnessed now at the surface.

We believe that XAFS has a lot more to offer to geoscientists for their understanding of the conditions at which petrogenesis develops. The number of synchrotron radiation sources where XAFS can be proficiently made is increasing rapidly, as are the beamlines optimized to investigate certain specific atoms i.e., suitable to exploit best the property that makes XAFS an invaluable tool in crystal chemistry, namely of investigating the environment around an atom and its electronic properties independently on any other atom present in any structural site, even those symmetry-equivalent to the very site assumed as the origin of the absorption process.

CALAS, G., MANCEAU, A. & PETIAU, J. (1988): Crystal chemistry of transition elements in minerals through X-ray absorption spectroscopy, 77-95. - In: Synchrotron radiation applications in mineralogy and petrology (S.S. Augusthitis, ed.). Athens, Theophrastus.

CHABOY, J. & QUARTIERI, S. (1995): X-ray absorption at the Ca K edge in natural-garnet solid solutions: a full-multiple-scattering investigation. - Phys. Rev. B52, 6349–6357.

CHOPIN,, C. (1984): Coesite and pure pyrope in high-grade blueschists of the Western Alps: a first record and some consequences. - Contrib. Mineral. Petrol., 86, 107–118.

DOBRZHINETSKAYA, L., GREEN, H.W.II & WANS, S. (1996): Alpe Arami: a peridotite massif from depths of more than 300 kilometers. - Science, 271, 1841–1845.

DURHAM, P.J., PENDRY, J.B. & HODGES, C.H. (1982): Calculation of X-ray absorption near-edge structure. - Comput. Phys. Commun., 25, 193–205.

FRICKE, H. (1920): K-characteristic absorption frequencies for the chemical elements magnesium to chromium. - Phys. Rev., 16, 202–215.

HEINRICH, C. (1986): Eclogite facies regional metamorphism of hydrous mafic rocks in the central alpine Adula nappe. - J. Petrol., 27, 123–154.

HERTZ G,. (1920): Über Absorptionslinien in Röntgenspektrum. - Phys. Z., 21, 630–632.

KRONIG, R.D.L. (1921): Zur Theorie der Feinstruktur in den Röngenabsorptionsspektren. - Z. Phys., 70, 317.

LEE, P.A. & PENDRY, J.B. (1975): Theory of extended x-ray absorption fine structure. - Phys. Rev., B11, 2795–2811.

MÖCKEL, J.R. (1969): Structural petrology of the garnet peridotite at Alpe Arami (Ticino), Switzerland. - Leidse Geol. Meded., 42, 61–130.

NATOLI, C.R., MISENER, D.K., DONIACH, S. & KUTZLER, F.W. (1980): First-principles calculation of X-ray absorption-edge structure in molecular cluster. - Phys. Rev., A22, 1104–1108.

NATOLI, C.R. & BENFATTO, M. (1986): A unifying scheme of interpretation of X-ray absorption spectra based on the multiple scattering theory. - J. Phys. (Paris), 47, C8, 11–23.

NATOLI, C.R., BENFATTO, M., BROUDER, C., RUIZ LOPEZ, M.Z. & FOULIS, D.L. (1990): Multichannel multiple-scattering theory with general potentials. - Phys. Rev., B42, 1944–1968.

PARIS, E., WU, Z., MOTTANA, A. & MARCELLI, A. (1995): Calcium environment in omphacitic pyroxenes: XANES experimental data versus one-electron multiple scattering calculations. - Eur. J. Mineral., 7, 1065–1070.

44